Title

A maternal-effect selfish genetic element in Caenorhabditis elegans

Journal

Science, 356(6342)

ISSN

0036-8075

Authors

Ben-David, Eyal

Burga, Alejandro

Kruglyak, Leonid

Publication Date

2017-06-09

DOI

10.1126/science.aan0621

Peer reviewed

HHS Public Access

Author manuscript

Science. Author manuscript; available in PMC 2018 November 24.

Published in final edited form as:

Science. 2017 June 09; 356(6342): 1051–1055. doi:10.1126/science.aan0621.

A maternal-effect selfish genetic element in *Caenorhabditis elegans*

Eyal Ben-David[#†], **Alejandro Burga**[#†], and **Leonid Kruglyak**[†]

Department of Human Genetics, Department of Biological Chemistry, and Howard Hughes Medical Institute, University of California, Los Angeles, Los Angeles, CA 90095, USA.

[#] These authors contributed equally to this work.

Abstract

Selfish genetic elements spread in natural populations and have an important role in genome evolution. We discovered a selfish element causing embryonic lethality in crosses between wild strains of the nematode *Caenorhabditis elegans*. The element is made up of *sup-35*, a maternal-effect toxin that kills developing embryos, and *pha-1*, its zygotically expressed antidote. *pha-1* has long been considered essential for pharynx development on the basis of its mutant phenotype, but this phenotype arises from a loss of suppression of *sup-35* toxicity. Inactive copies of the *sup-35/pha-1* element show high sequence divergence from active copies, and phylogenetic reconstruction suggests that they represent ancestral stages in the evolution of the element. Our results suggest that other essential genes identified by genetic screens may turn out to be components of selfish elements.

Selfish genetic elements subvert the laws of Mendelian segregation to promote their own transmission (1–5). In what is perhaps the most extreme scenario, selfish elements can kill individuals that do not inherit them, leading to genetic incompatibilities between carriers and non-carriers (5–9). Selfish elements are predicted to spread in natural populations (5, 6), and consequently, there is significant interest in using synthetic forms of such elements to drive population replacement of pathogen vectors in the wild (10, 11). However, despite the prominent role of selfish elements in genome evolution and their promise in pathogen control, their underlying genetic mechanisms have been resolved in only a few cases (5). Our laboratory previously identified a paternal-effect selfish element in the nematode *Caenorhabditis elegans* (12, 13). This element is composed of two tightly linked genes: *peel-1*, a sperm-delivered toxin, and *zeel-1*, a zygotically expressed antidote. In crosses between isolates that carry the element and ones that do not, the *peel-1* toxin is delivered by the sperm to all progeny, so that only embryos that inherit the element and the *zeel-1* antidote survive. An analogous element, Maternal-effect dominant embryonic arrest (*Medea*) has been previously described in the beetle *Tribolium*; however, the underlying genes remain unknown (8, 9).

[†]To whom correspondence should be addressed. ebd@ucla.edu (E.B); aburga@mednet.ucla.edu (A.B.); lkruglyak@mednet.ucla.edu (L.K.).

A maternal-effect genetic incompatibility in *C. elegans*

As part of ongoing efforts to study natural genetic variation in *C. elegans*, we introgressed a genetic marker located on the right arm of Chr. V from the standard laboratory strain N2 into the strain DL238 by performing eight rounds of backcrossing and selection. DL238 is a wild strain isolated in the Manuka Natural Reserve, Hawaii, USA, and is one of the most highly divergent *C. elegans* isolates identified to date (14). To confirm the success of the introgression, we genotyped the resulting strain at single-nucleotide variants (SNVs) between DL238 and N2 by whole-genome sequencing. As expected, with the exception of a small region on the right arm of Chr. V where the marker is located, most of the genome was homozygous for the DL238 alleles (Fig. 1A). However, to our surprise, we observed sequence reads supporting the N2 allele at many SNVs on Chr. III, including two large regions that were homozygous for the N2 allele despite the eight rounds of backcrossing (Fig. 1A, fig. S1). This observation suggested that N2 variants located on this chromosome were strongly selected during the backcrossing.

To investigate the nature of the selection, we performed a series of crosses between the N2 and DL238 strains and examined their progeny. To avoid effects of the *peel-1/zeel-1* element, which is present in N2 and absent in DL238, we performed a cross between DL238 males and a near isogenic line (NIL) that lacks the *peel-1/zeel*-1 element in an otherwise N2 background (hereafter, N2 *peel-1*$^{-/-}$) (13). We observed low baseline embryonic lethality in the F_1 generation and in the parental strains (0.26% ($N = 381$) for F_1; 0.99% ($N = 304$) for DL238; 0.4% ($N = 242$) for N2 *peel-1*$^{-/-}$), and we did not observe any obvious abnormal phenotypes in the F_1 that could explain the strong selection. However, when we allowed heterozygous F_1 hermaphrodites from this cross to self-fertilize, we observed 25.15% ($N = 855$) embryonic lethality among the F_2 progeny (Fig. 1B). Similar results were obtained for F1 hermaphrodites from the reciprocal parental cross (26.1%, $N = 398$). These results suggested the presence of a novel genetic incompatibility between N2 and DL238 that causes embryonic lethality in their F_2 progeny.

The observed pattern of embryonic lethality (no lethality in the parents nor in the F_1; 25% lethality in the F_2) is consistent with an interaction between the genotype of the zygote and a maternal or paternal effect (Fig. 1C) (12). We hypothesized that the incompatibility could stem from a cytoplasmically-inherited toxin that kills embryos if they lack a zygotically expressed antidote, analogous to the mechanism of the *peel-1/zeel-1* element (12, 13). To test this model and to discriminate between maternal and paternal effects, we crossed heterozygous F_1 DL238 × N2 *peel-1*$^{-/-}$ males and hermaphrodites with DL238 hermaphrodites or males, respectively (Fig. 1B, fig. S2). We observed 48.59% ($N = 389$) lethality when F_1 hermaphrodites were crossed to DL238 males, but only baseline lethality (1.17%; $N = 171$) in the reciprocal cross of F_1 males to DL238 hermaphrodites. 50% lethality when the F_1 parent is the mother and no lethality when the F1 parent is the father indicates that the incompatibility is caused by maternal-effect toxicity that is rescued by a linked zygotic antidote (fig. S2). We tested whether the new incompatibility was independent from the paternal-effect *peel-1/zeel-1* element by crossing DL238 and N2 worms and selfing the F_1 progeny. We observed 41.37% ($N = 389$) embryonic lethality

among the F_2 progeny, consistent with expectation for Mendelian segregation of two independent incompatibilities (43.75%) (Fig. 1D).

pha-1 and *sup-35* constitute a selfish element that underlies the incompatibility between DL238 and N2

To identify the genes underlying the maternal-effect incompatibility between N2 and DL238, we sequenced the genome of DL238 using Illumina short reads and aligned those reads to the N2 reference genome. We focused our attention on the two regions on Chr. III that were completely homozygous for the N2 allele in the introgressed strain (Fig. 1A, fig. S1). Inspection of short read coverage revealed a large ~E50 kb region on the right arm of the chromosome with very poor and sparse alignment to the N2 reference (Chr III: 11,086,500 – 11,145,000) (Fig. 2A). This region contains ten genes and two pseudogenes in N2. We noticed that *pha-1*, annotated as an essential gene in the reference genome, appeared to be completely missing in DL238 (Fig. 2A) (15). *pha-1* was originally identified as an essential gene required for differentiation and morphogenesis of the pharynx, the *C. elegans* feeding organ (15). But if *pha-1* is essential for embryonic development and missing in DL238, then how are DL238 worms alive? *pha-1* lethality can be fully suppressed by mutations in three other genes: *sup-35, sup-36*, and *sup-37* (16). We found no coding variants in *sup-36* and *sup-37* which reside on chromosomes IV and V, respectively (16) (fig. S3). However, *sup-35*, which is located 12.5kb upstream of *pha-1*, also appeared to be missing or highly divergent in DL238 (Fig. 2A, fig. S3).

We hypothesized that *sup-35* and *pha-1* could constitute a selfish element responsible for the observed incompatibility between the N2 and DL238 isolates. In our model, *sup-35* encodes a maternally-deposited toxin that kills embryos unless they express the zygotic antidote, *pha-1* (Fig. 2B). N2 worms carry the *sup-35/pha-1* element, which is missing or inactive in DL238, and F_1 hermaphrodites deposit the *sup-35* toxin in all their oocytes. 25% of their F_2 self-progeny do not inherit the element and are killed because they lack the antidote *pha-1*. Consistent with our model, an RNA-sequencing time-course of *C. elegans* embryogenesis showed that *sup-35* transcripts are maternally provided, whereas *pha-1* transcripts are first detected in the embryo at the 100-cell stage (17). To test our model, we first asked whether *sup-35* was necessary for the F_2 embryonic lethality in the N2 × DL238 cross. We crossed DL238 males to N2 *peel-1*$^{-/-}$ hermaphrodites carrying a null *sup-35(e2223)* allele (Fig. 2B). This *sup-35* allele was reported to fully rescue *pha-1* associated embryonic lethality (16). Embryonic lethality in the F_2 dropped from 25% to baseline in this cross (1.40%, $N = 576$), demonstrating that *sup-35* activity underlies the incompatibility between N2 and DL238 (Fig. 2B). We next tested whether expression of *pha-1*, the zygotic antidote, was sufficient to rescue the embryonic lethality. We introgressed a *pha-1* multicopy transgene into the DL238 and N2 *peel-1*$^{-/-}$ strains and repeated the cross. As predicted, expression of *pha-1* was sufficient to reduce embryonic lethality in the F_2 to baseline (1.49%, $N = 268$) (Fig. 2B). Moreover, we reasoned that if the *sup-35/pha-1* element underlies the maternal-effect lethality, arrested embryos from an N2 × DL238 cross should phenocopy *pha-1* mutant embryos. We collected rare L1-arrested F_2 larvae from an N2 *peel-1*$^{-/-}$ x DL238 cross and

observed major morphological defects in the pharynx of these individuals, as previously reported for *pha-1* mutants (15, 18) (Fig. 2C,D).

Together, these results show that *sup-35* and *pha-1* constitute a selfish element in *C. elegans*. Moreover, our results indicate that *pha-1* is not an organ-specific differentiation gene, as originally proposed (15), but a zygotically expressed antidote, and *sup-35* is a maternal-effect toxin rather than a suppressor of *pha-1*. This major reinterpretation of the roles of *pha-1* and *sup-35* is strongly supported by multiple lines of evidence from previous studies (18–21). First, *sup-35* overexpression phenocopies *pha-1* mutations, showing that *sup-35* is sufficient to cause embryonic lethality (19). Second, all defects associated with *pha-1* mutations are suppressed by mutations in *sup-35* (18–21). Third, when N2 hermaphrodites heterozygous for a deletion that includes both *sup-35* and *pha-1* (*tDf2/+)* self, the 25% of their progeny that are homozygous for this deletion arrest as embryos with pharyngeal defects (16, 19). Importantly, the lethality and pharyngeal defects of those homozygous embryos can be rescued by growing the heterozygous *tDf2/+* mother in *sup-35* RNAi, which depletes *sup-35* transcripts from the germline (20). These results indicate that maternally deposited *sup-35* is sufficient to kill embryos that lack *pha-1*, which is consistent with the role of *sup-35* as a maternal-effect toxin. Finally, whole genome sequence alignment across 26 nematode species indicates lack of *pha-1* conservation (Fig 2A). This observation is more consistent with its recent evolution as part of a selfish element in *C. elegans* than with its previously postulated role as a key developmental regulator (15).

Global variation in the activity of the *sup-35/pha-1* element

We examined the sequences of *sup-35* and *pha-1* in 152 *C. elegans* wild isolates that represented unique isotypes (22) in the *Caenorhabditis elegans* Natural Diversity Resource (23). Two isolates, QX1211 (California, USA) and ECA36 (Auckland, New Zealand), harbored a highly mutated copy of *pha-1*, with multiple non-synonymous SNVs as well as frameshifts expected to completely disrupt the protein (figs. S3 and S4). Both of these isolates also appeared to be missing *sup-35* (fig. S3). We predicted that these isolates should be incompatible with N2. Because QX1211 and ECA36 carry the same haplotype in the *sup-35*/*pha-1* region, we focused on further characterizing QX1211. We crossed QX1211 to N2 *peel-1*$^{-/-}$ worms and observed 23.9% (N = 355) lethality in the F_2 progeny, consistent with QX1211 carrying a degenerate copy of *pha-1*. Importantly, the lethality was abolished when we crossed QX1211 with N2 *sup-35(e2223); peel-1*$^{-/-}$ (0%, N = 290). Furthermore, we observed background levels of embryonic lethality (1.0%, N = 294) in the F_2 progeny of a DL238 × QX1211 cross, as expected, since both strains lack functional *sup-35*. Our analysis also revealed that the highly divergent Hawaiian isolate CB4856 carried a functional *sup-35*/*pha-1* element, which explains why previous studies did not detect it (12). Consistent with this observation, crossing the CB4856 and DL238 isolates led to the expected embryonic lethality in the F_2 (22.3%, $N = 349$).

We looked for additional variation in *sup*-35, *sup*-36, and *sup*-37 across the 152 isolates, which could potentially affect the activity of the *sup-35/pha-1* element (figs. S5-7). We found eight non-synonymous variants (three in *sup*-35, three in *sup*-36 and two in *sup-37)* and one premature stop codon in *sup-35* that removed 47% of the protein. We also identified

potential deletions by visually inspecting read alignments in each of the 152 isolates. While *sup-36* and *sup*-37 had consistent coverage in all isolates, we identified two structural variants in *sup*-35: a 530 bp deletion in the third intron, and a large 12.1 kb deletion that removed part of the last exon and the 3' UTR and fused *sup-35* to *Y48A6C.1*, a pseudogene that has partial homology with *sup-35*, creating a chimeric transcript (figs. S8 and S9). We tested strains carrying each of these variants for a maternal-effect lethality in crosses with DL238 (Table S2, fig. S10), and found that the lethality was completely abolished in strains carrying the chimeric *sup-35/Y48A6C.1* gene and in the strain carrying the premature stop codon in *sup-35*, indicating that these variants disrupt *sup-35* function. Thus loss of *sup-35* activity has occurred independently at least twice in carriers of N2-like alleles of the element.

DL238 and QX1211 carry an ancestral *sup-35/pha-1* haplotype

The alignment of DL238 and QX1211 short reads to the N2 reference genome was very sparse throughout the *sup-35/pha-1* region and at nearby genes, with some genes aligning only in exons and others not aligning at all (Fig. 2A). Moreover, several attempts to define the boundaries of the *pha-1* deletion in DL238 with diverse combinations of PCR primer pairs were unsuccessful. This suggested that the DL238 and QX1211 haplotypes were highly divergent from the N2 reference, and that major genomic rearrangements may have occurred. To resolve the genomic structure of the s*up-35/pha-1* element in these isolates, we *de novo* assembled the genomes of DL238 and QX1211 using a combination of our and previously published Illumina short reads (23, 24), followed by targeted Sanger sequencing to resolve repetitive regions and confirm scaffolds. The *de novo* assemblies confirmed that *pha-1* is absent from DL238 and is highly pseudogenized in QX1211, and that *sup-35* is pseudogenized in both (Fig. 3, fig. S11). DL238 and QX1211 share a very similar haplotype, with the exception of a large deletion in DL238 that encompasses *pha-1*, *fbxa-128* and several exons of *Y47D3A.1* (fig. S11). We also identified other large structural variants in both DL238 and QX1211 at the *sup-35/pha-1* locus. First, relative to the N2 reference genome, nearly 20kb of sequence is missing completely from both isolates (fig. S11). Second, the region spanning the pseudogenized *sup-35* and *Y48A6C.4* is inverted relative to the N2 reference (Fig. 3, fig. S11). This inversion was confirmed using single molecule Oxford Nanopore long-read sequencing (fig. S12). As a consequence of the inversion, the pseudogenized *sup-35* and *pha-1* are located next to each other in QX1211, rather than flanking *Y48A6C.4* as in the N2 reference genome (Fig. 3, fig. S11).

To gain further insights into evolution of the *sup-35/pha-1* element, we aligned the N2, DL238 and QX1211 haplotypes to the homologous regions of diverse *Caenorhabditis* species, using the highly conserved genes (*hmt-1*, *Y48A6C.4*, and *Y47D3A.29*) that delineated the region (Fig. 3, fig. S11). Unexpectedly, our analysis revealed that the order and orientation of these three genes in the other *Caenorhabditis* species matched that in DL238 and QX1211 rather than the order and orientation in N2. This observation suggests that the sup-35/pha-1 haplotype in DL238 and QX1211 derives from an early stage in the evolution of the selfish element, which was followed by a major inversion that now defines the N2 haplotype, and subsequent degeneration of the element in DL238 and QX1211. In further support of this model, a gene tree built using the coding region of *Y48A6C.4* from all

the *C. elegans* isolates and the other *Caenorhabditis* species showed that DL238, QX1211 and ECA36 cluster in a separate branch from all other *C. elegans* isolates (Fig. 3).

Discussion

We discovered a selfish genetic element in *C. elegans* that is composed of a maternally deposited toxin, *sup-35*, and a zygotically expressed antidote, *pha-1*. The antidote, *pha-1*, was originally thought to be a developmental gene, in large part due to the specific pharyngeal defects observed in mutants (15, 19, 25–27). However, the precise role of *pha-1* in embryonic development remained elusive and controversial (20, 21, 28). Our results indicate that *pha-1* pharyngeal defects are a direct consequence of *sup-35* toxicity, and that *sup-35* and *pha-1* act as a selfish element, instead of being integral components of *C. elegans* embryonic development as originally suggested.

One important insight emanating from previous work in light of our results is that the *sup-35/pha-1* element exerts its toxicity by recruiting genes that are directly involved in *C. elegans* development (16, 18–20, 26). The other two known suppressors of *pha-1* lethality, *sup-36* and *sup-37*, are essential for *sup-35* toxicity and are conserved in other nematodes (18, 20). Interestingly, *sup-37* is required for normal pharyngeal pumping and promotes ovulation in the somatic gonad independently of *pha-1* function (20). Null *sup-37* mutants are inviable and undergo early larval arrest. However, a single missense and viable mutation in *sup-37* is sufficient to abolish *sup-35* toxicity (18, 20). Together with the finding that SUP-37 physically interacts with SUP-35 (18), this suggests that the *sup-35/pha-1* selfish element is hijacking a developmental pathway to kill those embryos that do not inherit it. The specificity in the activity and expression of *sup-36* and *sup-37* may explain the pharyngeal phenotypes of *pha-1* mutants. We hypothesize that PHA-1 could act as an antidote by directly inhibiting the interaction between SUP-35 and SUP-37. The transcription factor *lin-35/Rb* and the E2 ubiquitin conjugation enzyme *ubc-18* downregulate *sup*-35 (19). An attractive possibility is that this regulation evolved as an additional mechanism to cope with *sup-35* toxicity, as part of an arms race between the selfish element and its host. Future studies may further resolve the mechanism of *sup-35* toxicity and its regulation.

One of the most intriguing aspects of toxin-antidote systems is their origin. The study of the *pha-1/sup-35* element provides some clues. *pha-1* has no known orthologs, and only a few highly divergent protein sequence matches are found in closely related *Caenorhabditis*. On the other hand, *sup-35* is a homolog of another *C. elegans* gene, *rmd-2*, which is conserved in other nematodes (19). A phylogenetic analysis shows that *sup-35* is more closely related to *C. elegans rmd-2* than to *rmd-2* genes from other species, and is likely a paralog of *rmd-2* (figs. S13 and S14). These results suggest that the origin of the *sup-35/pha-1* element involved the duplication of a pre-existing gene (*rmd-2*) and the recruitment of a novel gene of unknown origin in the lineage leading to *C. elegans*.

Among 152 *C. elegans* wild isolates examined, only DL238, QX1211, and ECA36 do not carry the derived inversion in the *sup-35/pha-1* element, and in all three of them, the selfish element is highly pseudogenized. Similar inversions have been described in the *Drosophila*

segregation distorter locus and in the mouse *t-haplotypes* (6, 29, 30), and are thought to stabilize two-component driver systems by preventing recombination from decoupling the components (6). Has the inversion facilitated the spread of *sup-35/pha-1* through the *C. elegans* population to all but few isolates? Ongoing efforts to identify more divergent isolates, as well as nematode species that are more closely related to *C. elegans*, may fill in the gaps in our understanding of the evolution of this element.

Lastly, our work highlights the importance of studying natural genetic variation for understanding gene function. Despite the indisputable value of a common reference strain, it has proved extremely difficult in the context of the N2 background alone to either confirm or rule out *pha-1* as an essential component of *C. elegans* embryonic development. The study of other wild isolates has made possible our characterization of *sup-35/pha-1* as a selfish element. Our results show that some essential genes may, in fact, turn out to be antidotes to unknown toxins. Selfish elements conferring genetic incompatibilities may be more common than previously thought, and some of them may be hiding in plain sight.

Supplementary Material

Refer to Web version on PubMed Central for supplementary material.

Acknowledgments:

We thank members of the Kruglyak lab for their comments. Funding was provided by the Howard Hughes Medical Institute and NIH grant R01 HG004321 (L.K.). E.B. is supported by a Gruss-Lipper postdoctoral fellowship from the EGL foundation. A.B. is supported by the Jane Coffin Childs Memorial Fund for Medical Research. E.B., AB. and L.K. wrote the manuscript. All authors discussed and agreed on the final version of the manuscript. The authors declare no competing financial interests. Sequencing data are available under NCBI bioproject PRJNA383603. Phylogenetic analyses have been deposited to TreeBASE (http://purl.org/phylo/treebase/phylows/study/TB2:S20933). The *liftoveR* R package has been deposited in Github (https://github.com/eyalbenda/liftoveR).

References and Notes

1. Dawkins R, The Selfish Gene (Oxford University Press, 1976).
2. Orgel LE, Crick FHC, Selfish DNA: the ultimate parasite. Nature. 284, 604–607 (1980). [PubMed: 7366731]
3. Doolittle WF, Sapienza C, Selfish genes, the phenotype paradigm and genome evolution. Nature. 284, 601–603 (1980). [PubMed: 6245369]
4. Sinkins SP, Invertebrate Post-Segregation Distorters: A New Embryo-Killing Gene. PLoS Biol. 9, e1001114 (2011). [PubMed: 21814492]
5. Werren JH, Selfish genetic elements, genetic conflict, and evolutionary innovation. Proc. Natl. Acad. Sci. U. S. A, 10863–70 (2011). [PubMed: 21690392]
6. Hurst GD, Werren JH, The role of selfish genetic elements in eukaryotic evolution. Nat. Rev. Genet 2, 597–606 (2001). [PubMed: 11483984]
7. Werren JH, Biology of Wolbachia. Annu. Rev. Entomol 42, 587–609 (1997). [PubMed: 15012323]
8. Lorenzen MD et al., The maternal-effect, selfish genetic element Medea is associated with a composite Tc1 transposon. Proc. Natl. Acad. Sci. U. S. A 105, 10085–9 (2008). [PubMed: 18621706]
9. Beeman R, Friesen K, Denell R, Maternal-effect selfish genes in flour beetles. Science. 256 (1992).
10. Chen C-H et al., A Synthetic Maternal-Effect Selfish Genetic Element Drives Population Replacement in Drosophila. Science. 316 (2007).

11. Hammond A et al., A CRISPR-Cas9 gene drive system targeting female reproduction in the malaria mosquito vector Anopheles gambiae. Nat. Biotechnol 34, 78–83 (2015). [PubMed: 26641531]
12. Seidel HS, Rockman MV, Kruglyak L, Widespread genetic incompatibility in C. elegans maintained by balancing selection. Science. 319, 589–94 (2008). [PubMed: 18187622]
13. Seidel HS et al., A novel sperm-delivered toxin causes late-stage embryo lethality and transmission ratio distortion in C. elegans. PLoS Biol. 9, e1001115 (2011). [PubMed: 21814493]
14. Andersen EC et al., Chromosome-scale selective sweeps shape Caenorhabditis elegans genomic diversity. Nat. Genet 44, 285–90 (2012). [PubMed: 22286215]
15. Schnabel H, Schnabel R, An Organ-Specific Differentiation Gene, pha-1, from Caenorhabditis elegans. Science. 250 (1990).
16. Schnabel H, Bauer G, Schnabel R, Suppressors of the organ-specific differentiation gene pha-1 of Caenorhabditis elegans. Genetics. 129 (1991).
17. Hashimshony T, Feder M, Levin M, Hall BK, Yanai I, Spatiotemporal transcriptomics reveals the evolutionary history of the endoderm germ layer. Nature. 519, 219–222 (2014). [PubMed: 25487147]
18. Polley SRG et al., Implicating SCF Complexes in Organogenesis in Caenorhabditis elegans. Genetics. 196 (2014).
19. Mani K, Fay DS, A Mechanistic Basis for the Coordinated Regulation of Pharyngeal Morphogenesis in Caenorhabditis elegans by LIN-35/Rb and UBC-18–ARI-1. PLoS Genet. 5, e1000510 (2009). [PubMed: 19521497]
20. Fay DS et al., A Regulatory Module Controlling Pharyngeal Development and Function in Caenorhabditis elegans. Genetics. 191 (2012).
21. Kuzmanov A, Yochem J, Fay DS, Analysis of PHA-1 Reveals a Limited Role in Pharyngeal Development and Novel Functions in Other Tissues. Genetics. 198 (2014).
22. Cook DE et al., The Genetic Basis of Natural Variation in Caenorhabditis elegans Telomere Length. Genetics. 204 (2016).
23. Cook DE, Zdraljevic S, Roberts JP, Andersen EC, CeNDR, the Caenorhabditis elegans natural diversity resource. Nucleic Acids Res. 45, D650–D657 (2017). [PubMed: 27701074]
24. van Schendel R et al., Polymerase Θ is a key driver of genome evolution and of CRISPR/Cas9-mediated mutagenesis. Nat. Commun 6, 7394 (2015). [PubMed: 26077599]
25. Granato M, Schnabel H, Schnabel R, Genesis of an organ: molecular analysis of the pha-1 gene. Development. 120, 3005–17 (1994). [PubMed: 7607088]
26. Fay DS et al., The coordinate regulation of pharyngeal development in C. elegans by lin-35/Rb, pha-1, and ubc-18. Dev. Biol 271, 11–25 (2004). [PubMed: 15196946]
27. Okkema PG, Ha E, Haun C, Chen W, Fire A, The Caenorhabditis elegans NK-2 homeobox gene ceh-22 activates pharyngeal muscle gene expression in combination with pha-1 and is required for normal pharyngeal development. Development. 124 (1997).
28. Mango SE, The Molecular Basis of Organ Formation: Insights From the *C. elegans* Foregut. Annu. Rev. Cell Dev. Biol 25, 597–628 (2009). [PubMed: 19575642]
29. Larracuente AM, Presgraves DC, The Selfish Segregation Distorter Gene Complex of Drosophila melanogaster. Genetics. 192 (2012).
30. Shin H-S, Flaherty L, Artzt K, Bennett D, Ravetch J, Inversion in the H–2 complex of t-haplotypes in mice. Nature. 306, 380–383 (1983). [PubMed: 6316154]
31. Agresti A, Coull BA, Approximate is better than “exact” for interval estimation of binomial proportions. Am. Stat 52, 119–126 (1998).
32. Pollard KS, Hubisz MJ, Rosenbloom KR, Siepel A, Detection of nonneutral substitution rates on mammalian phylogenies. Genome Res. 20, 110–21 (2010). [PubMed: 19858363]
33. Andersen EC et al., A Powerful New Quantitative Genetics Platform, Combining Caenorhabditis elegans High-Throughput Fitness Assays with a Large Collection of Recombinant Strains. G3 (Bethesda). 5, 911–20 (2015). [PubMed: 25770127]
34. Brenner S, The genetics of Caenorhabditis elegans. Genetics. 77, 71–94 (1974). [PubMed: 4366476]

35. Schedl T, Kimble J, fog-2, a germ-line-specific sex determination gene required for hermaphrodite spermatogenesis in Caenorhabditis elegans. Genetics. 119 (1988).
36. McKenna A et al., The Genome Analysis Toolkit: a MapReduce framework for analyzing next-generation DNA sequencing data. Genome Res. 20, 1297–303 (2010). [PubMed: 20644199]
37. Rimmer A et al., Integrating mapping-, assembly- and haplotype-based approaches for calling variants in clinical sequencing applications. Nat. Genet 46, 912–8 (2014). [PubMed: 25017105]
38. Garrison E, Marth G, Haplotype-based variant detection from short-read sequencing (2012) (available at http://arxiv.org/abs/1207.3907).
39. Koboldt DC et al., VarScan 2: Somatic mutation and copy number alteration discovery in cancer by exome sequencing. Genome Res. 22, 568–576 (2012). [PubMed: 22300766]
40. Wickham H, ggplot2: Elegant Graphics for Data Analysis (Springer-Verlag New York, 2009).
41. Hahne F, Ivanek R, in Methods in Molecular Biology (2016; http://link.springer.com/10.1007/978-1-4939-3578-9_16), vol. 1418, pp. 335–351. [PubMed: 27008022]
42. Langmead B, Trapnell C, Pop M, Salzberg SL, Ultrafast and memory-efficient alignment of short DNA sequences to the human genome. Genome Biol 10, R25 (2009). [PubMed: 19261174]
43. Li H, Durbin R, Fast and accurate long-read alignment with Burrows-Wheeler transform. Bioinformatics. 26, 589–595 (2010). [PubMed: 20080505]
44. Ou J, Wang Y, Zhu L, trackViewer: A bioconductor package with minimalist design for drawing elegant tracks or lollipop plot. R Packag. version 1.10.2, (available at https://bioconductor.org/packages/release/bioc/html/trackViewer.html).
45. Luo R et al., SOAPdenovo2: an empirically improved memory-efficient short-read de novo assembler. Gigascience. 1, 18 (2012). [PubMed: 23587118]
46. Altschul SF, Gish W, Miller W, Myers EW, Lipman DJ, Basic local alignment search tool. J. Mol. Biol 215, 403–410 (1990). [PubMed: 2231712]
47. Weisenfeld NI et al., Comprehensive variation discovery in single human genomes. Nat. Genet 46, 1350–1355 (2014). [PubMed: 25326702]
48. Loman NJ, Quinlan AR, Poretools: a toolkit for analyzing nanopore sequence data. Bioinformatics. 30, 3399–401 (2014). [PubMed: 25143291]
49. Darling AE, Mau B, Perna NT, progressiveMauve: multiple genome alignment with gene gain, loss and rearrangement. PLoS One. 5, e11147 (2010). [PubMed: 20593022]
50. Katoh K, Standley DM, MAFFT multiple sequence alignment software version 7: improvements in performance and usability. Mol. Biol. Evol 30, 772–80 (2013). [PubMed: 23329690]
51. Suyama M, Torrents D, Bork P, PAL2NAL: robust conversion of protein sequence alignments into the corresponding codon alignments. Nucleic Acids Res. 34, W609–12 (2006). [PubMed: 16845082]
52. Ronquist F, Huelsenbeck JP, MrBayes 3: Bayesian phylogenetic inference under mixed models. Bioinformatics. 19, 1572–4 (2003). [PubMed: 12912839]
53. Darriba D, Taboada GL, Doallo R, Posada D, jModelTest 2: more models, new heuristics and parallel computing. Nat. Methods 9, 772 (2012).
54. Yu G, Smith DK, Zhu H, Guan Y, Lam TT-Y, ggtree : an r package for visualization and annotation of phylogenetic trees with their covariates and other associated data. Methods Ecol. Evol 8, 28–36 (2017).

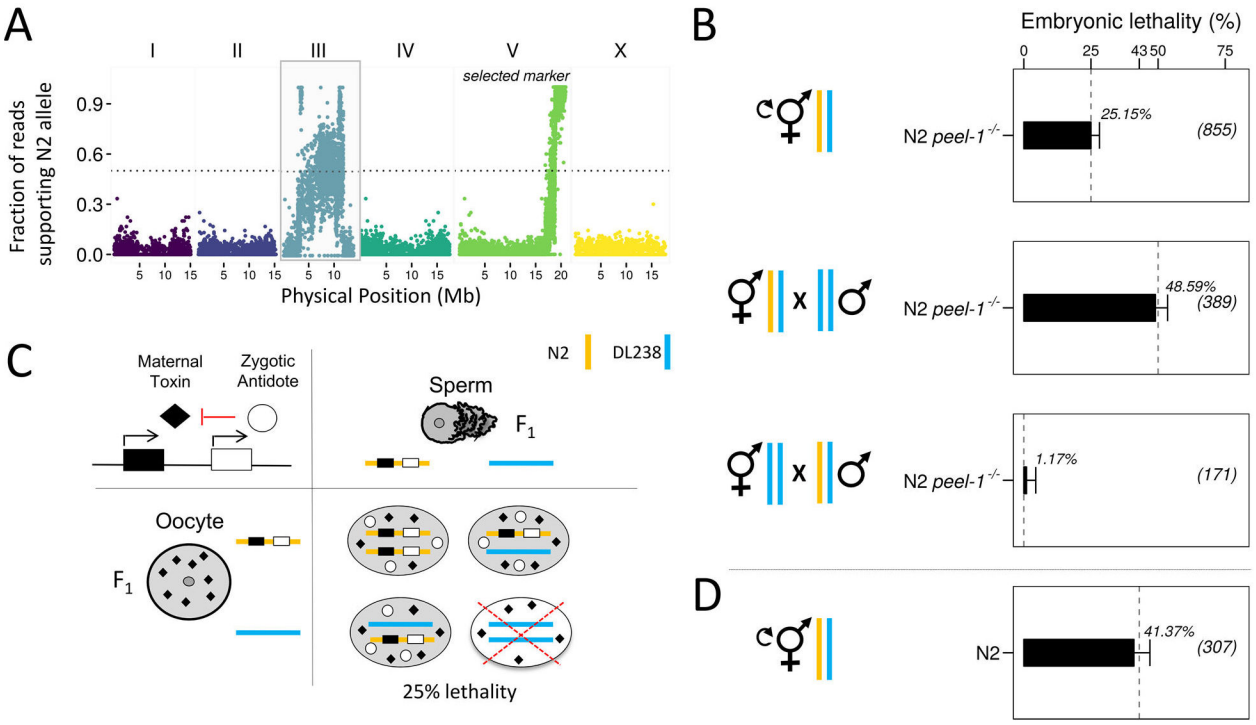

Fig 1. A maternal-effect genetic incompatibility on Chr. III.

(A) A marker on Chr. V was introgressed from the reference strain N2 into the DL238 wild isolate. Short-read sequencing of the introgression strain revealed homozygous N2 variants on Chr. III, indicating strong selection in favor of N2 variants during the generation of this strain. **(B)** DL238 males were crossed to hermaphrodites carrying a null allele of the *peel-1/zeel-1* element (*niDf9*) in an otherwise N2 background (N2 *peel-1*$^{-/-}$). F_1 hermaphrodites were allowed to self-fertilize (top). Alternatively, F_1 hermaphrodites (middle) or males (bottom) were backcrossed to the DL238 parental strain. Embryonic lethality was scored in the F_2 progeny as percent of unhatched eggs. Dashed grey lines indicate expected embryonic lethality under the maternal-effect toxin and zygotic antidote model (see also fig. S2). Sample sizes are shown in parentheses. Error bars indicate 95% binomial confidence intervals, calculated with the Agresti-Coull method (31) **(C)** Punnett square showing the expected lethality in the F_2. An interaction between a maternal toxin (black rhombus) and a zygotic antidote (white circle) results in 25% embryonic lethality in the F_2 and is compatible with the lethality observed in our crosses. **(D)** Embryonic lethality in the F_2 progeny of a cross between wild-type N2 hermaphrodites and DL238 males. N2 carries an active copy of *peel-1/zeel-1*, while DL238 carries an inactive copy. Independent segregation of two fully penetrant parental-effect incompatibilities is expected to result in 43.75% embryonic lethality. Orange and blue bars denote N2 and DL238 haplotypes, respectively.

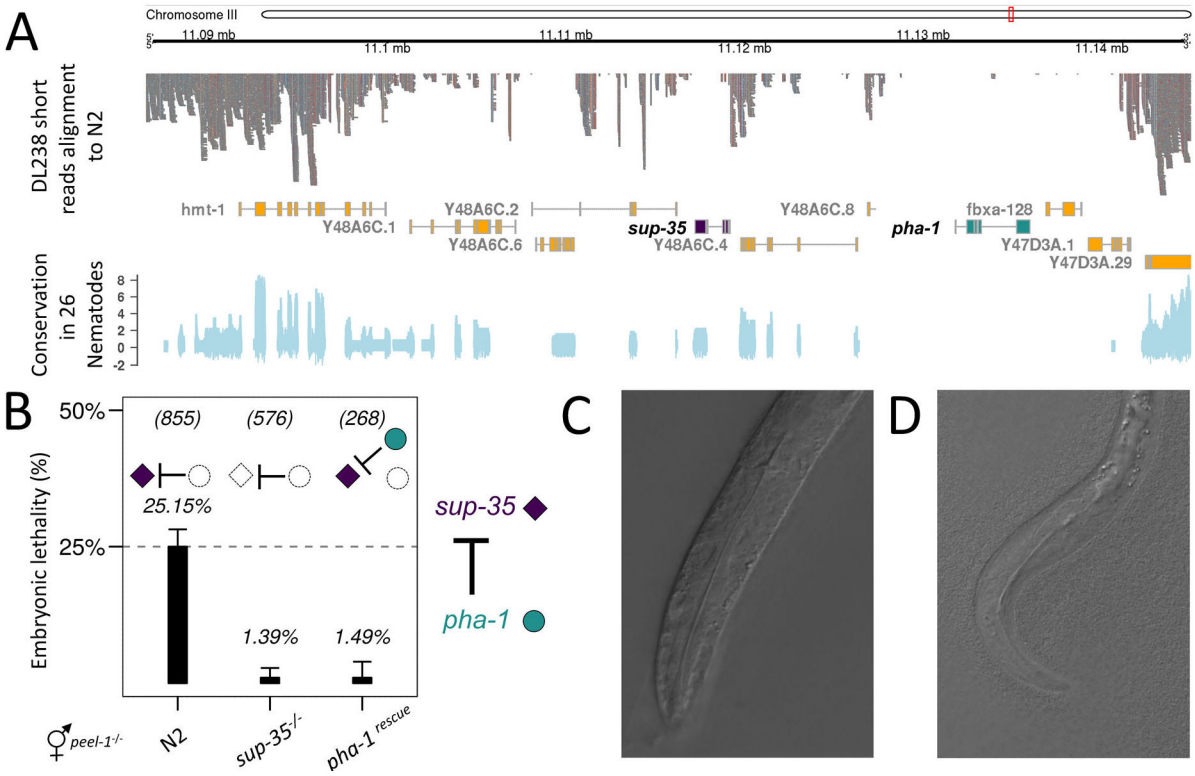

Fig 2. *sup-35* and *pha-1* encode a maternal-effect selfish genetic element.

(A) Alignment of short reads from DL238 to the N2 reference genome (top). A ~50kb region on the right arm of Chr. III selected during the introgression shows sparse alignment throughout with no read support for *pha-1* and weak support for *sup-35*. Whole genome sequence alignment across 26 nematode species (bottom). Values are *phyloP* scores retrieved from the UCSC genome browser (32) **(B)** In our model, *sup-35* is a maternally deposited toxin and *pha-1* is a zygotically expressed antidote. The embryonic lethality in the F_2 of the cross between DL238 and N2 *peel-1*$^{-/-}$ (left) was completely rescued when DL238 males were crossed to a strain carrying a *sup-35(e2223)* loss of function allele (center), and also when both parents carried a *pha-1* transgene (right). Error bars indicate 95% binomial confidence intervals, calculated using the Agresti-Coull method (31) **(C)** The pharynx of a phenotypically wild-type F_2 L1 worm from a DL238 × N2 *peel-1*$^{-/-}$*4* cross. **(D)** The pharynx of an F_2 L1 from the same cross as in (C) showing pharyngeal morphological defects and arrested development.

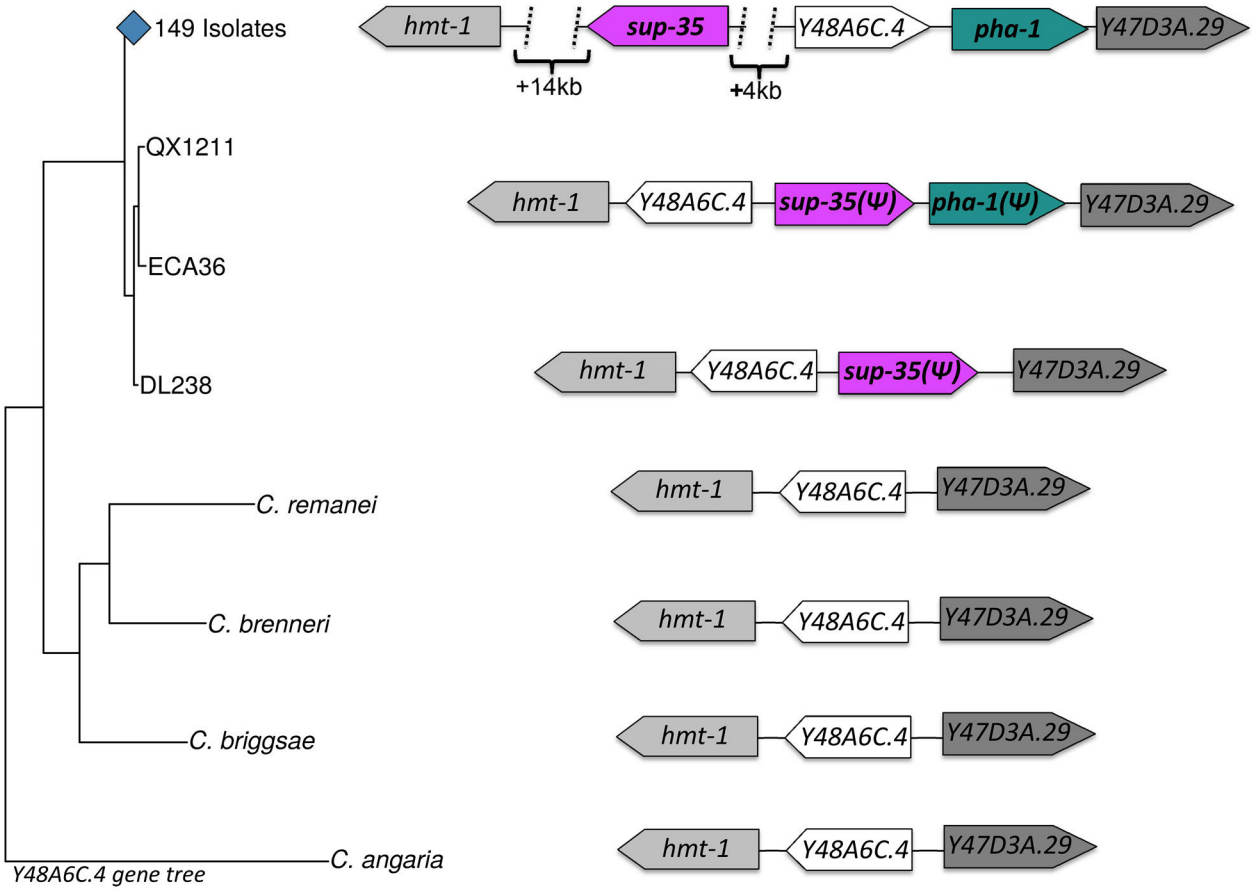

Fig 3. The *sup-35/pha-1* N2 haplotype is derived and is marked by an inversion.

(Left) A gene tree built using Bayesian inference from the coding region of *Y48A6C.4* in 152 *C. elegans* isolates and four other *Caenorhabditis* species. DL238, QX1211 and ECA36 cluster together in a separate branch from all other *C. elegans* isolates. (Right) The synteny in the region containing the *sup-35*/*pha-1* element, as well as three highly conserved genes in the close vicinity (*hmt-1, Y48A6C.4*, and *Y47D3A.29*) is schematically represented. ***(ψ)*** denotes alleles that are pseudogenized. The genes *sup-35* and *Y48A6C.4* are inverted in DL238, QX1211, and ECA36 relative to the other 149 *C. elegans* isolates. The gene order and orientation of *hmt-1, Y48A6C.4*, and *Y47D3A.29* in other *Caenorhabditis* species suggests that the inverted haplotype is the ancestral, and that the haplotype found in 149 isolates is the derived one.